FIFTH INTERNATIONAL CONGRESS ON SOUND AND VIBRATION

DECEMBER 15-18, 1997
ADELAIDE, SOUTH AUSTRALIA

DIRECT AND INVERSE SCATTERING OF PENETRABLE AND NONPENETRABLE OBSTACLES BY SHAPE DEFORMATION

D.N. Ghosh Roy†, Luise Couchman‡, and Jeremy Warner†

† SFA, Inc., 1401 McCormick Drive, Landover, MD 20785, USA
‡ Naval Research Laboratory, Code 7130, 4555 Overlook Ave,
Washington, DC 20735-5350, USA

The results of direct and inverse scattering of plane acoustic waves from impenetrable and penetrable objects are reported here. It is assumed that the scatterer boundary is a superposition of an arbitrary deformation on an underlying simple geometry. The direct problem is solved via the Padé extrapolation of the boundary variations. This results in solving only certain algebraic recursion relations and requires neither Green's function nor integral representations. The inverse problem of recovering the obstacle's shape and material parameters from the far-field scattering data is solved by Gauss-Newton minimization. The calculation of the scattered field and its Jacobian involves no more than solving a series of Helmholtz scattering problems in the same domain, namely, exterior to the simple shape instead of the iteratively updated deformed surfaces leading thereby to substantial computational simplifications. Finally, several two-dimensional obstacles of various shapes are inverted for their boundaries as well as their material parameters of mass density and wavenumber.

1 Introduction

The results of direct and inverse scattering of plane acoustic waves from Neumann and penetrating obstacles in a homogeneous, infinite medium are reported here. In the direct or forward problem, the obstacle is given and the objective is to determine how the plane wave is scattered by the object. In the inverse problem, on the other hand, it is the scattered field that is given, and the problem is to recover the scatterer (the boundary shape and the material parameters) from the given scattered field. In this paper it is assumed that the boundary of the scatterer can be described as a superposition of a deformation $\delta\Gamma$ (which may be finite) on a simple underlying geometry Γ_s which is considered to be known. It is further assumed that the magnitude of the deformation $\delta\Gamma$ is linearly proportional to some deforming function f. That is, $\delta\Gamma = \lambda f(\hat{\theta}), \lambda \in \mathbf{R}^1$, and $\hat{\theta} \in \mathbf{S}^2$, the unit sphere in $\mathbf{R}^3$. The solution of the forward problem makes use of this decomposition of the scatterer shape. The inverse solutions are obtained from the far-field patterns via the Gauss-Newton iteration procedure using the Levenberg-Marquardt nonlinear parameter estimation scheme. As is well-known, these procedures require that the forward problem be solved and the Jacobian of the scattered field (i.e., the derivative of the scattered field with respect to a suitably chosen parameterization of the boundary) be determined at every stage of the iteration. The formalism discussed here particularly addresses these two crucial questions. More details appear in [1]. It is assumed that the penetrable scatterers are homogeneous in their material parameters, which are the mass density ρ and the wavenumber k.

2 Description of the Method

The solution of the direct problem basically consists of two steps: the determination of the scattered field assuming a slight perturbation (λ small) of the underlying simple shape Γ_s, and then extrapolating the result to the actual, finite variation of the boundary (λ not necessarily small). Here, we consider scattering in two space dimensions only, for which Γ_s is assumed to be a circle Γ_c of radius r_0. The decomposition of the scatterer boundary is then given by $r(\theta) = r_0 + \lambda f(\theta), \theta \in [0, 2\pi]$ (see Figure 1). $f(\theta)$ is the function that deforms the circle and is represented by a finite Fourier series, namely, $f(\theta) = \sum_{l=-L}^{L} \alpha_l e^{il\theta}, \alpha_l = \alpha^*_{-l}$, where * denotes complex conjugation.

For $|x| > \max_{\theta\in[0,2\pi]} |r_0 + \lambda f(\theta)|$, the scattered field is expanded in terms of the outgoing wavefunctions, namely

$$\psi^{sc}(x; \lambda, f) = \sum_{m=-\infty}^{\infty} \gamma_m(\lambda, f)(-i)^m H_m^{(1)}(k_0|x|)e^{im\theta}, \tag{1}$$

where $H_m^{(1)}$ is the Hankel function of the first kind of order m. Also, for small values of λ, ψ^{sc} can be expanded in a Taylor series [2]

$$\psi^{sc}(x; \lambda, f) = \sum_{m=0}^{\infty} \frac{1}{m!} \psi^{(m)}(x, f)\lambda^m = \sum_{m=0}^{\infty} \tilde{\psi}^{(m)}(x)\lambda^m. \tag{2}$$

$\tilde{\psi}^{(0)}$ corresponds to scattering for the undeformed circle Γ_c. It can be shown [1, 2] that $\tilde{\psi}^{(m)}$ can be obtained for all m by solving the same Helmholtz scattering problem as that

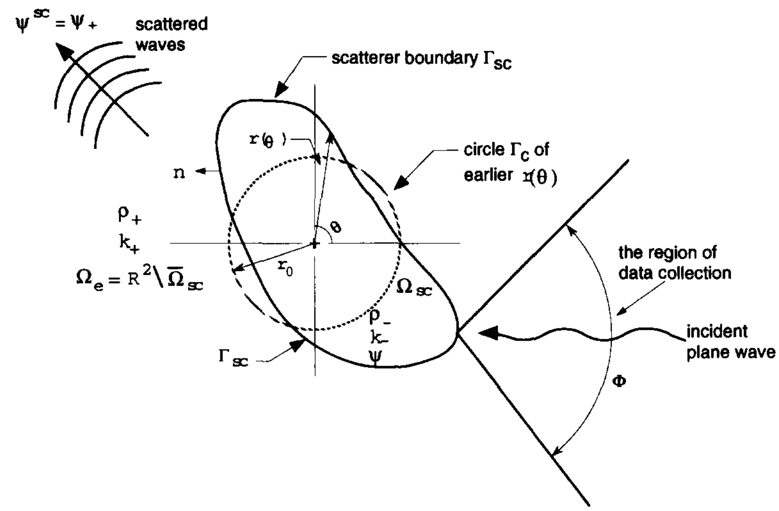

Figure 1. The geometry of scattering of a plane acoustic wave from an obstacle. The scatterer shape is given by $r(\theta) = r_0 + \lambda f(\theta), \theta \in [0, 2\pi]$. $\Phi_0 \leq \Phi \leq 2\pi, \Phi_0 > 0$. For a Neumann object the interior wavenumber k_- vanishes.

of the forward problem in the domain exterior to Γ_c, but with different boundary data that depend recursively on $\tilde{\psi}^{(p)}$, $p < m$. Moreover, on the circle Γ_c, the coefficients $\tilde{\psi}^{(m)}$ admit of the Rayleigh expansion

$$\tilde{\psi}^{(m)}(x) = \sum_{z=-\infty}^{\infty} \beta_{m,z}(-i)^z H_z^{(1)}(k_0|x|)e^{iz\theta}. \tag{3}$$

The coefficients $\beta_{m,z}$ are obtained by making use of Eq. (3) and the boundary data for $\tilde{\psi}^{(m)}$ on Γ_c. Since the $\tilde{\psi}^{(m)}$'s are determined recursively, then so are the $\beta_{m,n}$'s. Finally, the coefficients γ_m in Eq. (1) are related to the coefficients $\beta_{m,n}$ of Eq. (3) as

$$\gamma_m = \sum_{n=-\infty}^{\infty} \beta_{m,n}\lambda^n. \tag{4}$$

The above relations hold only for small values of λ. However, for a finite deformation, that is, when λ is beyond the radius of convergence of the Taylor series (2), ψ^{sc} is calculated by extrapolating the Taylor series by the Padé approximation [3].

Note that all calculations refer only to Γ_c and not to the deformed surface of the scatterer. This is particularly significant from the viewpoint of the inverse solution since in a Gauss-Newton iteration process, the scatterer boundary is continuously updated. This fact together with the form of the recursion relations for $\beta_{m,n}$ (see Section 4) introduces substantial simplifications in the computation of the Jacobian. As pointed out earlier, the Levenberg-Marquardt algorithm requires the knowledge of the Jacobian, the determination of which accounts for the major portion of the computation time. It can be shown [1] that using the methodology of this paper, the computation of the full Jacobian involves no more than solving a single, albeit extended, forward problem in the domain exterior to Γ_c. Therefore, the domain in which the scattering problem is solved in order to determine the Jacobian remains independent of the stage of iteration. This is a crucial point.

3 Results

The main results consist of the recursion relations for $\beta_{m,n}$, which are written below for the Neumann and transmission problems.

Neumann Scatterer

The exterior Neumann boundary value problem in $\Omega_e = \mathbf{R}^2 \backslash \bar{\Omega}_{sc}$ is given by

$$(\Delta + k^2)\psi = 0 \quad \text{in} \quad \Omega_e$$

$$\frac{\partial \psi}{\partial n}|_{\Gamma_{sc}} = 0$$

$$\psi = \psi^{sc} + \psi^{inc}$$

$$\lim_{|x| \to 0} (\frac{\partial \psi^{sc}}{\partial |x|} - ik\psi^{sc}) = o(|x|^{-1})$$

The recursion relation for $\beta_{m,n}$ is

$$\beta_{m,n} = -\frac{k^m}{H_n^{(1)}(\xi)} \sum_{i=1}^{4} T_i^{m,n} \tag{5}$$

where the $T_i^{m,n}$ are defined as

$$T_1^{m,n} = \sum_{l=-Lm}^{Lm} (-i)^l \alpha_{m,l} J_{n-l}^{(m+1)}(\xi),$$

$$T_2^{m,n} = \sum_{j=0}^{m-1} \sum_{l=-Lm}^{Lm} \frac{(-i)^l(-1)^j(1+j)}{(m-j-1)!} \frac{l(n-l)}{\xi^{2+j}} \alpha_{m,l} J_{n-l}^{(m-j-1)}(\xi),$$

$$T_3^{m,n} = \sum_{j=0}^{m-1} \sum_{l=-L(m-j)}^{L(m-j)} (-i)^l \frac{1}{k^j} \alpha_{m-j,l} \beta_{j,n-l} H_{n-l}^{(m-j+1)}(\xi),$$

and

$$T_4^{m,n} = \sum_{j=0}^{m-1} \sum_{p=0}^{m-j-1} \sum_{l=-L(m-j)}^{L(m-j)} (-i)^l (-1)^p (1+p) l(n-l) \frac{(m-j-1)!}{(m-j-p)!} \cdot$$

$$\cdot \frac{1}{k^j \xi^{2+p}} \alpha_{m-j,l} \beta_{j,n-l} H_{n-l}^{(m-j-p-1)}(\xi).$$

The argument ξ of the Bessel and Hankel functions stands for kr_0, and $\alpha_{p,l}$ is the l^{th} Fourier coefficient in the expansion of the p^{th} power of the deformation function $f(\theta)$. Moreover, $\zeta_p^{(q)} = \frac{d^q \zeta_p}{d\xi^q}$, where ζ_p is either J_p or H_p.

Penetrable Scatterer

The scattering problem for penetrable scatterers is

$$
\begin{aligned}
(\Delta + k_+^2)\psi_+ = 0 \quad &\text{in} \quad \Omega_e = \mathbf{R}^2 \backslash \bar{\Omega}_{sc} \\
(\Delta + k_-^2)\psi_- = 0 \quad &\text{in} \quad \Omega_{sc} \\
\frac{\partial \psi_+}{\partial n} = \frac{\rho_+}{\rho_-}\frac{\partial \psi_-}{\partial n} \quad &\text{on} \quad \Gamma_{sc} \\
\psi_+ = \psi_- \quad &\text{on} \quad \Gamma_{sc}
\end{aligned}
$$

For the transmission problem, we have two sets of coefficients, one for the interior and one for the exterior region. The following two recursion relations apply for the penetrable obstacles.

$$
\beta^+_{m,n} k_+ H_n^{(1)}(\xi_+) - \beta^-_{m,n}\rho_0 k_- J_n^{(1)}(\xi_-) = \sum_{i=1}^{4} R_i^{m,n} \tag{6}
$$

and

$$
\beta^+_{m,n} H_n(\xi_+) - \beta^-_{m,n} J_n(\xi_-)\beta_{m,n} = \sum_{i=1}^{2} S_i^{m,n} \tag{7}
$$

where in Eq. (6) the $R_i^{m,n}$ are defined as

$$
R_1^{m,n} = \frac{k_+^{m+1}}{m!}\sum_{l=-Lm}^{Lm} (-i)^l \alpha_{m,l} J_{n-l}^{(m+1)}(\xi_+),
$$

$$
R_2^{m,n} = \sum_{j=0}^{m-1}\sum_{l=-Lm}^{Lm} \frac{(-i)^l(-1)^j(1+j)}{(m-j-1)!}\frac{l(n-l)}{\xi^{2+j}}\alpha_{m,l} J_{n-l}^{(m-j-1)}(\xi_+),
$$

$$
R_3^{m,n} = \sum_{j=0}^{m-1}\sum_{l=-L(m-j)}^{L(m-j)} (-i)^l \frac{1}{k^j}\alpha_{m-j,l}\Lambda^{m-j+1},
$$

and

$$
R_4^{m,n} = \sum_{j=0}^{m-1}\sum_{p=0}^{m-j-1}\sum_{l=-L(m-j)}^{L(m-j)} (-i)^l(-1)^p(1+p)l(n-l)\frac{(m-j-1)!}{(m-j-p)!}\cdot
$$

$$
\cdot\frac{1}{k^j\xi^{2+p}}\alpha_{m-j,l}\Lambda^{m-j-p-1},
$$

where

$$
\Lambda^n = \beta^+_{j,n-l} k_+^n H_{n-l}^{(n)}(\xi_+) - \beta^-_{j,n-l}\rho_0 k_-^n J_{n-l}^{(n)}(\xi_-).
$$

Similarly for Eq. (7), the $S_i^{m,n}$ are defined as

$$
S_1^{m,n} = \frac{k_+^m}{m!}\sum_{l=-Lm}^{Lm} (-i)^l \alpha_{m,l} J_{n-l}^{(m)}(\xi_+),
$$

and

$$
S_2^{m,n} = \sum_{j=0}^{m-1}\sum_{l=-L(m-j)}^{L(m-j)} (-i)^l \alpha_{m-j,l}(\beta^+_{j,n-l} k_+^{m-j} H_{n-l}^{(m-j)}(\xi_+) - \beta^-_{j,n-l} k_-^{m-j} J_{n-l}^{(m-j)}(\xi_-)).
$$

In this notation, k_+, k_- are the exterior and the interior wavenumber, respectively. Also, $\xi_\pm = r_0 k_\pm$. $\beta^-_{m,n}$ refers to the coefficients for the scatterer, and $\beta^+_{m,n}$ are the coefficients of the ambient medium.

Solving $\beta^+_{m,n}$ from the coupled systems (6) and (7), replacing it in Eq. (4), Padé extrapolating and finally, using the expansion (1) then solves the transmission problem.

4 Main Features of the Method

The method presented above has three essential features which are significant when solving the inverse problem. First, all calculations refer only to the circle Γ_c and not to the actual boundary shape which undergoes continuous updating in a Gauss-Newton inversion. Secondly, the recursion relations for the coefficients $\beta_{m,n}$ are such that the determination of the full Jacobian of the scattered field (the knowledge of which is required in the minimization process) amounts to solving a series of Helmholtz scattering problems in the same domain (which is $\Omega_e = \mathbf{R}^2 \backslash \bar{\Omega}_{sc}$) with different boundary data. This is to be contrasted to that of solving these scattering problems in distinctly different domains, one for each of the Fourier coefficients in the Fourier parameterization of the boundary Γ_{sc}. This results in a significant simplification in the calculation of the Jacobian which accounts for most of the computing time. (More details on this point appear in [1]). Thirdly, since the $\beta_{m,n}$'s are determined by solving a set of algebraic recursion relations that involve neither Green's function nor any integral representation of the scattered field, the nonuniqueness resulting from the interior eigenvalues of the corresponding adjoint Dirichlet problem [4] does not arise.

References

[1] Ghosh Roy, D.N., Couchman, L., and Warner, J. (1997): Scattering and inverse scattering of sound-hard obstacles via shape deformation *Inverse Problems*, **13**, 585-606

[2] Bruno, O.P. and Reitich, F. (1995): A new approach to the solution of problems of scattering by bounded obstacles *SPIE*, **2192**, 20-8

[3] Baker, G.A. and Graves-Morris, P. (1981): *Padé Approximants. Part I: Basic Theory* (Reading, MA: Addison-Wesley)

[4] Colton, D. and Kress, R. (1992): *Inverse Acoustic and Electromagnetic Scattering Theory* (New York: Springer)

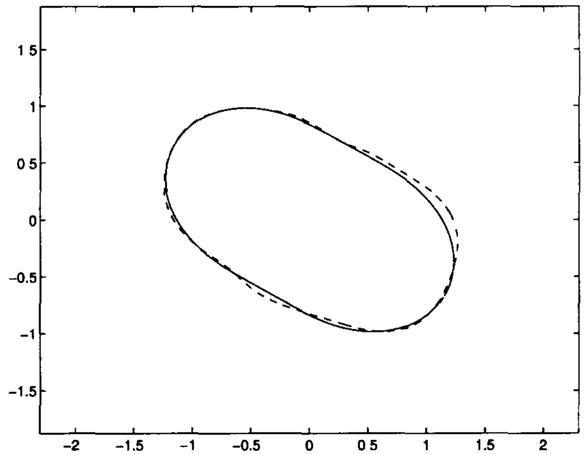

Figure 2a

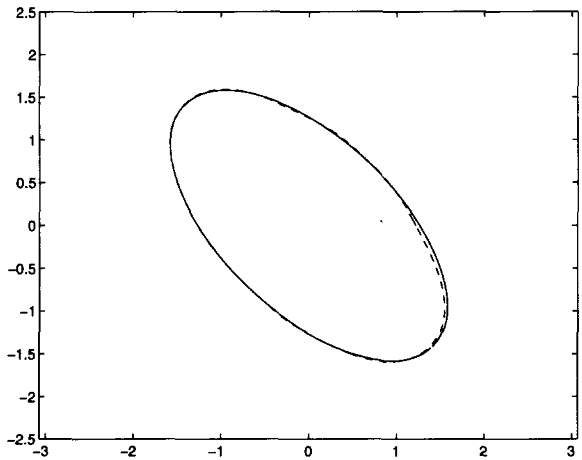

Figure 2b

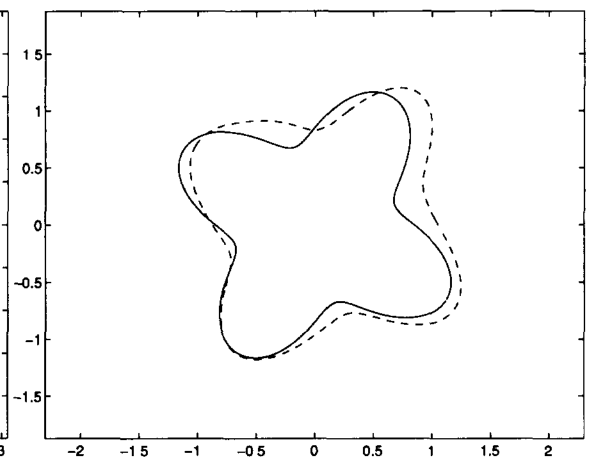

Figure 2c

Figure 2. Reconstructions of boundary for sound-hard objects from the far-field data. a) Sausage: $r(\theta) = 1 + 0.3\cos(2\theta) + 0.03\cos(4\theta)$ from 90^o wedge of data (that is, $\Phi = 90^o$ in Figure 2). Number of frequencies used = 3, and the number of unknown Fourier coefficients = 17. b) A 2.0:1.0 ellipse from full-cycle data using 3 frequencies, and 17 unknown Fourier coefficients. c) Cloverleaf: $r(\theta) = 1 + 0.3\cos(4\theta)$ from 15^o wedge of data using 41 frequencies, no noise, and 17 unknown Fourier coefficients. Figures (2a) and (2b) have 8% noise added to the data. —— actual shape, - - - reconstructed shape.

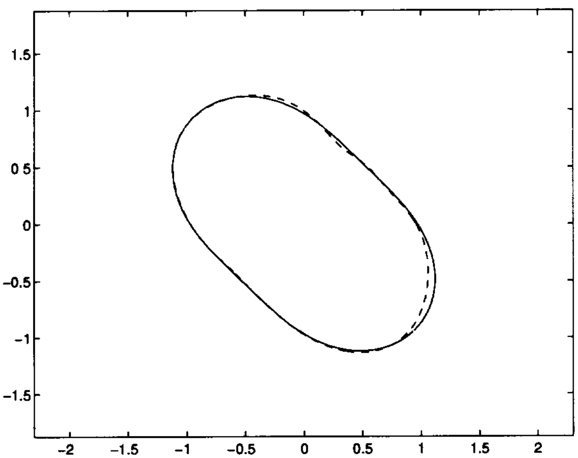

Figure 3a

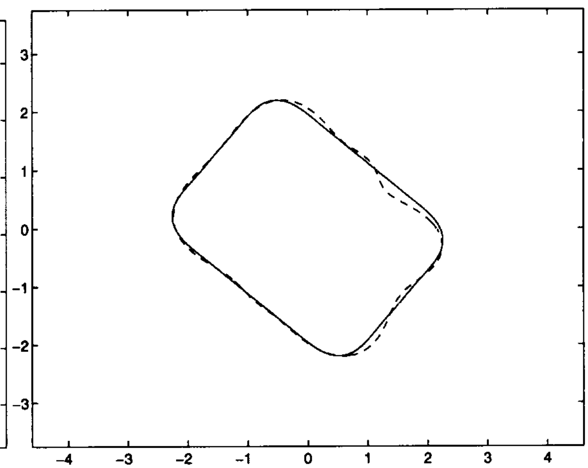

Figure 3b

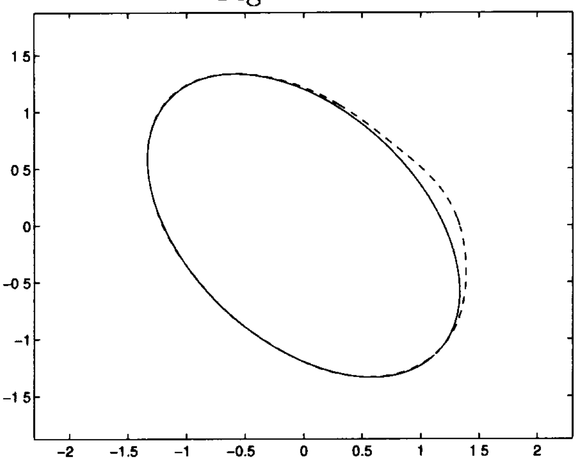

Figure 3c

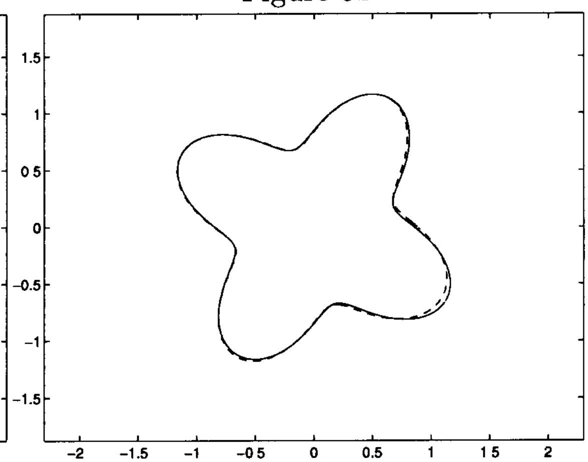

Figure 3d

Figure 3. Reconstructions of the shapes of some penetrable objects from the far-field data. a) Sausage: $r(\theta) = 1 + 0.3\cos(2\theta) + 0.03\cos(4\theta)$ $\kappa_t = 3.00, \rho_t = 0.500; \kappa_i = 1.50, \rho_i = 0.800; \kappa_f = 3.34, \rho_f = 0.483$. b) A 4.0x3.0 Box with rounded corners $\kappa_t = 3.00, \rho_t = 0.250; \kappa_i = 1.00, \rho_i = 1.00; \kappa_f = 2.33, \rho_f = 0.237$. c) A 1.6:1.0 Ellipse $\kappa_t = 4.00, \rho_t = 0.333; \kappa_i = 1.00, \rho_i = 1.00; \kappa_f = 3.47, \rho_f = 0.336$. d) Cloverleaf: $r(\theta) = 1 + 0.3\cos(4\theta)$ $\kappa_t = 2.00, \rho_t = 0.500; \kappa_i = 1.00, \rho_i = 1.00; \kappa_f = 2.02, \rho_f = 0.520$. The reconstructions used full-cycle data, three frequencies, 17 unknown Fourier coefficients, and with 8% random noise. Here $\kappa = k_+/k_-$ and $\rho = \rho_+/\rho_-$. The subscripts t, i, f refer to the true, initial, and final values, respectively. —— actual shape, - - - reconstructed shape.